Published in final edited form as:
J Chem Neuroanat. 2012 March ; 43(2): 103–111. doi:10.1016/j.jchemneu.2011.11.002.

Descending projections from the rostral ventromedial medulla (RVM) to trigeminal and spinal dorsal horns are morphologically and neurochemically distinct

Sue A. Aicher[*], **Sam M. Hermes**, **Kelsey L. Whittier**, and **Deborah M. Hegarty**
Department of Physiology & Pharmacology, Oregon Health & Science University, 3181 Sam Jackson Park Road, Portland, OR 97239-3098

Abstract

Neurons in the rostral ventromedial medulla (RVM) are thought to modulate nociceptive transmission via projections to spinal and trigeminal dorsal horns. The cellular substrate for this descending modulation has been studied with regard to projections to spinal dorsal horn, but studies of the projections to trigeminal dorsal horn have been less complete. In this study, we combined anterograde tracing from RVM with immunocytochemical detection of the GABAergic synthetic enzyme, GAD67, to determine if the RVM sends inhibitory projections to trigeminal dorsal horn. We also examined the neuronal targets of this projection using immunocytochemical detection of NeuN. Finally, we used electron microscopy to verify cellular targets. We compared projections to both trigeminal and spinal dorsal horns. We found that RVM projections to both trigeminal and spinal dorsal horn were directed to postsynaptic profiles in the dorsal horn, including somata and dendrites, and not to primary afferent terminals. We found that RVM projections to spinal dorsal horn were more likely to contact neuronal somata and were more likely to contain GAD67 than projections from RVM to trigeminal dorsal horn. These findings suggest that RVM neurons send predominantly GABAergic projections to spinal dorsal horn and provide direct input to postsynaptic neurons such as interneurons or ascending projection neurons. The RVM projection to trigeminal dorsal horn is more heavily targeted to dendrites and is only modestly GABAergic in nature. These anatomical features may underlie differences between trigeminal and spinal dorsal horns with regard to the degree of inhibition or facilitation evoked by RVM stimulation.

Keywords

Descending modulation; GABA; GAD67; confocal microscopy; electron microscopy

1. Introduction

The rostral ventromedial medulla (RVM) is a critical site for descending modulation of nociceptive transmission (Fields et al., 1983; Fields and Basbaum, 1978; Heinricher et al., 1989; Sandkühler and Gebhart, 1984). Neurons in RVM are thought to produce

[*]Corresponding author: aichers@ohsu.edu, Phone: 503.418.2550, Fax: 503.494.4352.

Conflict of interest statement: There are no conflicts of interest.

antinociception through inhibitory projections to the dorsal horn (Heinricher et al., 1994). RVM stimulation produces both antinociception and reduces activity of dorsal horn neurons in response to noxious stimuli (Fields et al., 1977; Haber et al., 1980; Sandkühler and Gebhart, 1984). However, an anatomical substrate for this inhibition has not been firmly defined (Fields et al., 1995; Kalyuzhny and Wessendorf, 1999). Recent reviews suggest that inhibition of nociceptive transmission could be mediated by axoaxonic modulation of primary afferent input to the superficial dorsal horn; modulation of postsynaptic projection neurons; or modulation of interneurons within the dorsal horn (Millan, 2002). The present neuroanatomical studies directly address the cellular mechanisms by which RVM neurons may modulate the transmission of nociceptive information through the spinal and trigeminal dorsal horn.

Previous neuroanatomical and electrophysiological studies have suggested that descending inhibitory projections from RVM to various levels of spinal cord are serotonergic, glycinergic and GABAergic. However, the relative contribution of these projections to the inhibition of nociceptive transmission in the spinal and trigeminal dorsal horns remains unclear. Many neurons in RVM contain a synthetic enzyme of GABA, glutamic acid decarboxylase (GAD) (Jones et al., 1991; Millhorn et al., 1987; Winkler et al., 2006). We previously used retrograde tracing methods to show that approximately 50% of RVM neurons with projections to the cervical spinal dorsal horn contain the GAD67 isoform and likely provide descending inhibition to the dorsal horn (Morgan et al., 2008). However, these retrograde tracing studies did not demonstrate the precise distribution of the descending fibers from RVM or their cellular targets in spinal cord. In the current studies, we used biotinylated dextran amine (BDA) to anterogradely trace projections from the RVM to both the lumbar spinal and trigeminal dorsal horns. Using this anterograde tract tracing method combined with GAD67 immunocytochemistry and confocal microscopy, we have verified the relative proportion of GABAergic fibers projecting from RVM to the dorsal horns at both trigeminal and spinal levels. We also combined anterograde tracing with detection of NeuN to determine if RVM projections to dorsal horn target neuronal cell bodies. By conducting further electron microscopic analyses, we have also determined that the cellular targets of the projections from RVM are primarily dendrites of neurons in the outer laminae of both spinal and trigeminal dorsal horns.

2. Materials and Methods

2.1. Experimental animals and surgery

All protocols were approved by the Institutional Animal Care and Use Committee at Oregon Health & Science University and conform to the European Union Directive 2010/63/EU for animal experimentation. Male Sprague-Dawley rats (n = 11; 290-350 g; 8 – 12 weeks of age; Charles River Laboratories) were housed in pairs on a 12/12 Light/Dark cycle and were given access to food and water ad libitum. To trace projections from the RVM to trigeminal and spinal dorsal horns, each rat was anesthetized with 5% isoflurane in oxygen from an Isotec Tec3 vaporizer (Datex-Ohmeda; Madison, WI). The head was shaved and disinfected, then the rat was positioned into a David Kopf stereotaxic frame (Tujunga, CA) with a nose cone for anesthesia delivery (2-3% isoflurane in oxygen). The anterograde tracer BDA (10% solution of 10k molecular weight in 0.1 M phosphate buffer (PB); Invitrogen, Carlsbad, CA) was utilized to trace medullary projections to the trigeminal and spinal dorsal horns. The brain was accessed by drilling a hole through the skull with a dental drill (Aseptico; Woodinville, WA) and removing a small section of dura. Stereotaxic coordinates for RVM were measured from the interaural line (midline, 2.3 mm caudal and 11.6 mm ventral). BDA (50 – 65 nl) was pressure-injected using single-barrel glass micropipettes. Following injections, micropipettes were left in place for 5 minutes before removal. Surgical incisions were closed with 3-0 monocryl suture (Ethicon; Cornelia, GA) and coated in antibiotic

ointment. The rat was removed from anesthesia, monitored during recovery and subsequently returned to the colony.

2.2. Perfusion and tissue preparation

Survival times following injections varied depending on whether or not transport to the lumbar spinal cord was to be evaluated. Survival times for rats that were only evaluated at the trigeminal region ranged between 2 and 7 days (n = 8), while rats that were evaluated at both the trigeminal and lumbar regions ranged from 11 to 12 days (n = 3) to allow sufficient time for the BDA to be transported to the lumbar spinal cord. The total number of BDA-labeled varicosities in the trigeminal dorsal horn of animals who survived 2 to 7 days was compared to the number in animals who survived 11 to 12 days using a t-test. Survival time did not affect the total number of BDA-labeled varicosities observed in the trigeminal dorsal horn (t-test, $p = 0.16$, SigmaStat, Systat Software, Inc., San Jose, CA). Rats were overdosed with sodium pentobarbital (150 mg/kg) and perfused transcardially through the ascending aorta. Each rat was perfused with 10 ml of heparinized saline (1000 units/ml), followed by 50 ml of 3.8% acrolein in 2% paraformaldehyde, and 200 ml of 2% paraformaldehyde in 0.1 M PB, pH 7.4. The caudal trigeminal brainstem, lumbar enlargement of the spinal cord, and RVM were removed and placed in 2% paraformaldehyde for 30 min. Tissue blocks were placed into 0.1 M PB and the brainstem and spinal cord (L2 – L5) were sectioned at 40 μm (RVM injection sites were sectioned at 60 μm) on a vibrating microtome (Leica, Malvern, PA). Prior to immunocytochemical processing, free floating tissue sections were placed in 1% $NaBH_4$ (Sigma-Aldrich, St. Louis, MO) for 30 min to bind remaining free aldehydes, and then in 0.5% bovine serum albumin (BSA; Sigma-Aldrich) in 0.1 M Tris-buffered saline (TS) for 30 minutes to reduce nonspecific binding.

2.3. Dual labeling for BDA and either GAD67 or NeuN

Adjacent sections through the regions of interest were processed for dual-labeled immunofluorescence or for combined immunoperoxidase and immunogold labeling for electron microscopy. Sections chosen for immunofluorescent analysis were processed for detection of BDA as well as either GAD67 (Millipore, Temecula, CA), one isoform of the enzyme necessary for GABA synthesis, or NeuN (Millipore), a neuronal marker. Immunofluorescence studies were performed as previously described (Aicher et al., 2000; Bailey et al., 2006; Winkler et al., 2006). Briefly, tissue sections were incubated in a primary monoclonal mouse antibody directed against either GAD67 (1:2000), or NeuN (1:2000) for 48 hours at 4°C with continuous agitation. Following rinsing, tissue sections were incubated with a cocktail containing a donkey α mouse secondary antibody conjugated to AlexaFlour 647 (Invitrogen, Carlsbad, CA; 1:800) and streptavidin conjugated to AlexaFluor 488 (Invitrogen; 6.25 μg/ml) for 2 hours at room temperature. All primary and secondary antibodies were made in a 0.1% BSA (Sigma-Aldrich) solution in 0.1 M TS; 0.25% Triton X-100 (Sigma-Aldrich) was also added to primary antibody solutions. All incubations were performed with continuous agitation at room temperature unless otherwise noted and all steps after and including secondary antibody incubation were protected from ambient light. Tissue sections were mounted on gelatin-coated slides, coverslipped with ProLong Gold™ Antifade reagent (Invitrogen) and stored at -20°C.

2.4. Specificity of Antibodies

The monoclonal mouse anti-GAD67 antibody (MAB5406, clone 1G10.2, Millipore) recognizes the N-terminal region (amino acid residues 4-101) of a recombinant human GAD67(Bottger et al., 2011; Fong et al., 2005; Guo et al., 2010) and does not cross-react with the GAD65 isoform by Western blot of rat cortex (Fong et al., 2005). Immunoblot results in a single 67 kDa band, omission controls produced no labeling, and immunohistochemical detection in brainstem neurons was verified using in situ

hybridization (Fong et al., 2005). In addition, an overall decrease in GAD67 immunolabeling using this antibody was found in the cortex and striatum of mutant mice in which the *Gad1* gene was conditionally knocked out in dopamine receptor 1-expressing medium spiny neurons, as compared to control mice (Heusner et al., 2008). The monoclonal mouse anti-NeuN antibody (NEUronal Nuclei, MAB377, clone A60, Millipore) recognizes the DNA-binding, neuron-specific protein NeuN and was raised against purified cell nuclei from mouse brain (Mullen et al., 1992). Immunocytochemical studies indicate that this antibody recognizes the nuclei of most neurons, except for Purkinje cells, mitral cells and photoreceptor cells, among others, and does not label glial cell types (Bottger et al., 2011; Mullen et al., 1992). This antibody recognizes three bands in the 46-48 kDa range in immunoblots on mouse brain nuclear proteins, but not nuclear proteins from other mouse tissues such as heart, liver and thymus.

2.5. Electron Microscopy

Tissue sections destined for electron microscopy underwent immunoperoxidase labeling for BDA and immunogold labeling with silver enhancement for GAD67 (Aicher et al., 1995; Chan et al., 1990). Briefly, following immersion in 1% $NABH_4$ as described above, sections were immersed in cryoprotectant solution (25% sucrose, 3% glycerol in 0.05 M PB) for 30 minutes and then briefly immersed in Freon followed by liquid nitrogen. This “freeze-thaw” method increases penetration of antibodies into the surface of the tissue with a minimal disruption of morphology. BDA was then visualized with the avidin-biotin detection method (Hsu et al., 1981). This was followed with a 30 minute incubation in 0.5% BSA (Sigma) and a 48 hour incubation at 4°C in mouse anti-GAD67 (1:500, Millipore) primary antibody in 0.1% BSA (Sigma-Aldrich) in 0.1 M TS. No Triton X-100 was utilized. After rinses, tissue sections were then incubated with a goat anti-mouse IgG conjugated to colliodal gold (Ultra-Small; 1:50, Electron Microscopy Sciences (EMS), Hatfield, PA) for 2 hours at room temperature. Sections were rinsed in citrate buffer and colloidal gold particles were enhanced by silver intensification for 6 minutes using the IntenSE™ M kit (GE Healthcare Life Sciences, Buckinghamshire, UK) (Chan et al., 1990). All incubations, except the primary antibody incubation, were carried out at room temperature with continuous agitation and sections were rinsed between incubations in 0.1 M TS.

Following the dual-labeling immunoperoxidase and immunogold procedure, tissue sections were fixed for 1 hour in 2.0% osmium tetroxide in 0.1 M PB, washed for 10 min in 0.1 M PB, dehydrated through a graded series of ethanols, then propylene oxide, and then placed in a 1:1 mixture of propylene oxide and EMBed 812 (EMS) solution overnight. Sections were then incubated in EMBed 812 for 2 hours, embedded between two sheets of Aclar plastic (Ted Pella, Redding, CA), and placed in an oven for 24 to 48 hours at 60°C.

Regions of the trigeminal and dorsal horn that contained both labels were glued to plastic blocks formed in Beem capsules (Ted Pella) (Pickel, 1981) and ultrathin sections (75 nm) through the outer surface of the tissue were collected onto copper grids. The thin sections were counterstained with uranyl acetate and Reynolds lead citrate and examined using an FEI Tecnai 12 electron microscope (Hillsboro, OR).

2.6. Data analysis for confocal microscopy

Images were collected utilizing a Plan-Apochromat 40× / 1.4 NA oil objective on a Zeiss LSM 510 META confocal microscope (Carl Zeiss MicroImaging, Thornwood, NY) using the single pass, multi-tracking format of the Zeiss LSM 510 META or ZEN software. One track was utilized to collect emissions from AlexaFluor 488 after excitation with a 488 nm (Argon/2) laser and a 500-550 nm band pass filter. A second track captured emissions from AlexaFluor 647 after excitation with a 633 nm laser (HeNe2) and a 650-710 nm band pass

filter. Consecutive and overlapping 0.5 μm thick optical sections were captured as Z stacks bounded by the vertical extent of labeling. For trigeminal dorsal horn analyses, both the right and left sides of the ventrolateral trigeminal subnucleus caudalis (Vc) at its transition zones with subnucleus interpolaris (rostral Vi/Vc) and cervical spinal cord (caudal Vc/C1) were scanned in each animal. Additionally, confocal images were captured for each side of lumbar spinal cord from one section in each animal. Sections were chosen for analysis based on the following criteria: (1) The presence of anatomical landmarks visible under darkfield illumination that are hallmarks of the Vi/Vc and Vc/C1 transition zones and the lumbar spinal cord dorsal horn, such as fiber tracks, shape of the lumbar spinal cord gray matter and the appearance of the substantia gelatinosa; and (2) the coincidence of BDA-labeled fibers in these segments of the trigeminal brainstem and lumbar spinal cord. Only cases with optimal morphology that contained the labels of interest were included in the analyses. BDA-labeled varicosities were operationally defined as approximately circular manifestations along fibers that were at least twice the diameter of the parent fiber (Bailey et al., 2006). Varicosities were identified and numbered on optical slices known to contain either GAD67 or NeuN immunoreactivity. However, at the time of identification, those respective channels were turned off to ensure random sampling. Criteria for co-localization of BDA-labeled terminals with GAD67 was similar to our previous studies (Mitchell et al., 2004a; Silverman et al., 2005). Specifically, GAD67 immunoreactivity had to be included entirely within the BDA-labeled varicosity in at least two consecutive 0.5 μm thick optical sections. For apposition analysis with NeuN immunoreactivity, the BDA-labeled varicosity had to be directly adjacent to a NeuN-immunoreactive (-ir) profile for two consecutive optical sections as well. All co-localization and appositional analyses of BDA-labeled varicosities were verified by independent blinded observers. To minimize sampling bias, only one varicosity was randomly selected per axon, but varicosities from all axons within each scan were counted. The proportions of dual-labeled varicosities containing both BDA and GAD67 immunoreactivity to total BDA-labeled varicosities in Vc/C1 were compared to the proportions in Vi/Vc by using the z-test, in which high z values indicated that the proportions of the two groups were different and in which p values less than 0.05 were considered significant. We also performed z-tests to compare the proportions of BDA-labeled varicosities that were apposed to NeuN-labeled cells to total BDA-labeled varicosities in Vc/C1 and Vi/Vc (SigmaStat) (Hegarty et al., 2010). Chi Square tests were performed to evaluate differences between confocal counts made in the trigeminal dorsal horn versus the dorsal horn of the lumbar spinal cord (SigmaStat). Confocal micrographs used for publication are projections of one or several optical sections that were adjusted for optimal brightness and contrast.

2.7. Ultrastructural Analysis of Reticulomedullary and Reticulospinal Targets

Ultrastructural analyses were conducted on plastic-embedded sections from six animals that were selected from an area just below the surface of the tissue at the tissue/plastic interface, where the penetration of antibodies is optimal (Aicher et al 1995, Aicher et al 1999). Only regions of tissue containing both immunogold and immunoperoxidase markers within 25 μm of each other were analyzed. An average of 1000 μm^2 was examined in the trigeminal dorsal horn of each animal; 700 μm^2 in the lumbar dorsal horn of each animal. All areas that contained both immunoperoxidase-labeled terminals and immunogold-labeled profiles, somata, dendrites, axons, axon terminals or glia, were photographed. Positive immunogold identification of profiles was dependent on the minimum cross-sectional diameter. Profiles with a minimum cross-sectional diameter between 0 and 1.0 μm^2 were considered positive for immunogold labeling if they contained at least two gold particles, profiles between 1.1 and 2.0 μm^2 had to contain at least three gold particles, and profiles larger than 2.1 μm^2 had to contain at least four gold particles. A Fisher Exact test was performed to evaluate whether

reticulospinal terminals that contacted dendrites had the same likelihood of being GABAergic as those that made contacts with non-dendritic targets (SigmaStat).

3. Results

3.1. Injection Sites

Injections of BDA into mid-line RVM resulted in bilateral anterograde labeling in both the trigeminal and lumbar spinal dorsal horns (Figure 1). BDA injection sites in the RVM were visualized with the avidin-biotin reaction described above. All injections impinged on the RVM (n = 11, Figure 1A,B) and resulted in bilateral labeling in the trigeminal (Figure 1C) or spinal dorsal horn (Figure 1D). BDA-labeled axons and varicosities were located in the outer laminae throughout the rostrocaudal extent of the trigeminal (Figure 1C) and lumbar spinal dorsal horns (Figure 1D). Confocal and electron microscopic analyses were confined to laminae I and II.

3.2. Reticulospinal varicosities are more likely to contain GAD67 immunofluorescence than reticulomedullary varicosities

In the trigeminal dorsal horn, a total of 315 BDA-labeled varicosities were identified from 8 animals (bilateral observations from the Vi/Vc and Vc/C1 transition areas from each animal), with an average of 39 ± 5 (SEM) varicosities per animal. There were no differences in the proportions of BDA-labeled varicosities that contained GAD67 immunoreactivity to total varicosities in Vc/C1 and Vi/Vc (z-test, $p = 0.297$), therefore, the numbers from these two regions were pooled as trigeminal dorsal horn data. A subset, 29% (90 out of 315), of BDA-labeled varicosities in the trigeminal dorsal horn were immunoreactive for GAD67 (Figure 2A-C). This is lower than our previous observations that approximately half the neurons in RVM that we identified by retrograde tracing from the cervical spinal cord contained GAD67 (Morgan et al., 2008), raising the possibility that there may be differences between the trigeminal brainstem and the spinal cord.

Since most other studies examined RVM projections to and from lumbar spinal cord rather than trigeminal dorsal horn, we examined anterograde fibers to lumbar dorsal horn in a subset of animals. In contrast to our findings in trigeminal dorsal horn, we found a much higher proportion of RVM projections to lumbar spinal dorsal horn contained GAD67 (Chi Square, $p < 0.001$). We examined 74 varicosities in the lumbar dorsal horn (n= 3; 25 ± 4 varicosities per animal with bilateral observations from a single section per animal). A majority of these varicosities, 61% (45 of 74), contained GAD67 immunoreactivity. This is substantially greater than the 29% of GAD67-ir varicosities found in trigeminal dorsal horn projecting fibers in 8 animals (see above), but closer to that seen previously in cervical spinal cord (Morgan et al., 2008) .

The three animals examined for the studies in lumbar spinal dorsal horn were also among those animals that were examined for studies in trigeminal dorsal horn. For these three animals, 23% (29 of 126) of BDA-containing varicosities in trigeminal dorsal horn contained GAD67 immunoreactivity, which is consistent with the 29% of GAD67-ir BDA-containing varicosities found in the trigeminal dorsal horns of all 8 animals (see above). This indicates that the differences between reticulospinal (61% in 3 animals) and reticulomedullary (29% in 8 animals; 23% in 3 animals) GAD67-ir BDA-containing varicosities are consistent, even within the same animal. This finding indicates that the location of the injection sites between animals does not account for the differences in GAD67 content between trigeminal and lumbar projections.

3.3. RVM projections are more likely to contact NeuN immunofluorescent neuronal somata in lumbar than trigeminal dorsal horn

In order to determine whether RVM projections might target postsynaptic neurons in the dorsal horn, we used NeuN immunoreactivity to identify neurons in the trigeminal and spinal dorsal horns and counted the number of BDA-labeled varicosities that were apposed to neuronal targets. In trigeminal dorsal horn, a total of 374 BDA-labeled varicosities were identified from 8 animals (bilateral observations from the Vi/Vc and Vc/C1 transition areas from each animal), with an average of 47 ± 9 varicosities per animal. There were no differences in the proportions of BDA-labeled varicosities that apposed NeuN-labeled cells to total varicosities in Vc/C1 and Vi/Vc (z-test, $p = 0.247$), therefore, the numbers from these two regions were pooled as trigeminal dorsal horn data. We found that 28% (106 out of 374) of the identified axonal varicosities (13 ± 4 varicosities per animal) in the trigeminal dorsal horn formed appositions with NeuN-ir cells (Figure 3A-C). In the lumbar spinal dorsal horn, 36 varicosities were identified from 3 animals (12 ± 3 varicosities per animal, bilateral observations per animal) and 60% (22 out of 36, 7 ± 3 per animal) were found to be apposed to NeuN-ir cells. These findings suggest a strong axosomatic projection from RVM to the spinal, but not trigeminal, dorsal horn (Chi Square, $p < 0.001$). These findings are consistent with the GAD67 analysis above, based on observations in many brain regions that somatic synaptic inputs are often GABAergic. Specifically, RVM projections to lumbar spinal cord, which are more often GABAergic, are also more frequently in close apposition to somata. While this confocal analysis suggests the presence of direct synapses between RVM axon terminals and neurons within the spinal and trigeminal dorsal horns (Figure 3A-C), the presence of direct synaptic input to dorsal horn neurons can only be verified by electron microscopy. We found that indeed, RVM axon terminals do form direct symmetric synaptic contacts with neuronal perikarya (Figure 3D).

3.4. Ultrastructurally identified reticulomedullary projections contain GABA and target dendrites

Our confocal analyses above showed that one-third and two-thirds of RVM axon terminals appear to form axosomatic contacts with neurons in the trigeminal and spinal dorsal horn, respectively. However, the nature of the neuronal targets for the other axon terminals could not be determined by the confocal analysis. Therefore, we conducted electron microscopic analyses to determine if RVM axon terminals form axodendritic, axosomatic, or axoaxonal contacts in the trigeminal (n = 5 animals) and spinal (n = 3 animals) dorsal horns. This analysis was conducted largely on a subset of animals with anterograde labeling to both trigeminal and lumbar dorsal horns. These data are summarized in Table 1.

A total of 51 BDA-labeled axon terminals were identified in the trigeminal dorsal horn (10 ± 2 terminals per animal). Most (65%; 33 of 51) BDA-labeled axon terminals contained GAD67 immunoreactivity regardless of the type of postsynaptic target. In addition, the majority (69%; 35 of 51) of the BDA-labeled axon terminals contacted dendrites (Figure 4A, B). Of the BDA-labeled axon terminals that contact dendrites, 71% (25 of 35) of these axon terminals contained GAD67 immunoreactivity.

The majority of the dendritic targets, 96% (49 of 51) were unlabeled and presumed to be non-GABAergic neurons (Figure 4). The remaining 4% of dendritic targets contacted by BDA-labeled axon terminals contained GAD67 (2 of 51) (Figure 5A). Some BDA-labeled axon terminals were only apposed to astrocytic glial processes in the plane of section examined (Figure 5B).

We found GAD67-ir axons to be abundant in spinal and trigeminal dorsal horns (Figure 5C), and these axons were often in close proximity to other GAD67-ir axons and unlabeled axon

terminals. However, we did not find axoaxonic contacts between GAD67-ir axon terminals and BDA-labeled axon terminals arising from RVM.

3.5. Ultrastructurally identified reticulospinal projections contain GABA and target dendrites

A total of 36 BDA-labeled axon terminals were identified in the lumbar dorsal horn (12 ± 2 terminals per animal). Like the trigeminal region, most of the BDA-labeled terminals (56%; 20 of 36) in the lumbar dorsal horn contacted dendrites. A subset, 60% (12 of 20), of the BDA-labeled axon terminals that contacted dendrites also contained GAD67 immunoreactivity (Figure 4C). The likelihood of BDA-labeled axon terminals containing GAD67 immunoreactivity was the same whether the axon terminals contacted dendrites (60%), or any other targets (69%, 11 of 16; Fisher's exact; $p = 0.731$). Only 10% (2 of 20) of dendrites contacted by BDA-labeled axon terminals contained GAD67 immunoreactivity.

A BDA-labeled axon terminal contacted a neuronal somata in the plane of section examined (Figure 5D). The rare observance of axosomatic contacts at the electron microscopic level is likely influenced by the very small region of analysis in any electron microscopic study and the high ratio of dendritic processes per perikaryon in the neuropil of the dorsal horn.

Overall, the ultrastructural data confirm that somatic and dendritic profiles are contacted by GABAergic axon terminals arising from the RVM. The findings are consistent at both trigeminal and lumbar spinal levels. The restricted number of profiles examined at the ultrastructural level limits the ability to directly compare results quantitatively to the confocal analyses above. Furthermore, with sampling restricted to regions that contained both markers within 25 μm of each other, we may be biasing samples to regions with higher GAD67 immunoreactivity in the ultrastructural studies.

4. Discussion

The present findings support previous observations that descending RVM projections target neurons in the dorsal horn, rather than primary afferent axons. We found that by confocal analysis, RVM projections to lumbar spinal dorsal horn more frequently contain GAD67 and contact neuronal somata, compared to RVM projections to trigeminal dorsal horn. At both levels, the primary targets of RVM projections are somata and dendrites of dorsal horn neurons. Previous studies have speculated that GABAergic inputs to primary afferent fibers may arise from descending pathways (Millan, 2002), but the present studies do not support that notion. Our findings are consistent with previous anatomical studies indicating that descending pathways from RVM to spinal dorsal horn target postsynaptic neurons in the dorsal horn (Antal et al., 1996; Light and Kavookjian, 1985). We did not determine if these neurons are interneurons or projection neurons, but the absence of GAD67 in the dendritic targets of most RVM axon terminals indicates that the targets are not likely to be inhibitory interneurons.

We did find evidence of presynaptic GABAergic axon terminals in contact with other unlabeled axon terminals in dorsal horn, which is consistent with previous studies (Alvarez et al., 1992). Alvarez and colleagues report GABAergic presynaptic axon terminals may selectively modulate subsets of primary afferents, such as high-threshold A-delta fibers identified in their study (Alvarez et al., 1992). They and others failed to demonstrate GABAergic presynaptic afferents to unmyelinated or peptidergic nociceptive afferents (Alvarez et al., 1993; Ruda et al., 1986). Alvarez and colleagues conclude that the GABAergic terminals making axoaxonic contacts with identified primary afferents likely arise from local inhibitory interneurons, rather than descending projections (Alvarez et al., 1992). Our studies support this conclusion and indicate that the GABAergic terminals that

form synaptic contacts with other GABAergic and unlabeled terminals in the dorsal horn do not arise from descending projections from RVM.

The prevalence of GAD67-ir BDA varicosities was greater in lumbar than trigeminal dorsal horn, suggesting that descending GABAergic modulation of nociceptive input to the dorsal horn may be less robust in trigeminal pathways as compared to lumbar spinal pain processing. This difference in GABAergic modulation may be due to the vulnerability of specialized sensory tissues that are innervated by the trigeminal nerve and whose sensory information is processed in the trigeminal dorsal horn, such as ocular and oral structures and nasal membranes (Bereiter et al., 2000; Hargreaves, 2011; Meng and Bereiter, 1996; Pozo and Cervero, 1993; Strassman and Vos, 1993). The trigeminal dorsal horn may receive less of a GABAergic descending inhibitory input in order to facilitate the protective role of acute pain in alerting the organism of impending injury to a sensory system that is critical to the organism's survival. Our trigeminal analysis was confined to the ventrolateral region of Vc, which receives afferent input from the ophthalmic branch of the trigeminal nerve. This area contains afferents from nociceptive tissues such as the cornea, and appears to be modulated by descending input from RVM (Meng et al., 2000). Our present studies did not determine if the anatomical arrangements in the ophthalmic region of Vc would generalize to other afferent branches of the trigeminal nerve, particularly those that are not involved in nociceptive processing.

Many studies have reported descending facilitation following RVM stimulation (Urban et al., 1999; Zhuo and Gebhart, 1990), and the degree of facilitation or inhibition produced by RVM stimulation can be altered in various pain states. Previous studies have reported variations in descending modulation between spinally innervated body segments such as tail and foot (Fang and Proudfit, 1996), and a recent study showed that inactivation of the RVM by local injection of bupivacaine differentially interfered with pain modulation from the RVM to the trigeminal and spinal levels (Edelmayer et al., 2009). RVM inactivation completely blocked dural inflammation-induced mechanical allodynia as measured from the forehead, while mechanical allodynia was only partially and temporarily attenuated in the plantar hind paw at the time points measured (Edelmayer et al., 2009). These studies and our results suggest that descending modulation from RVM to trigeminal and spinal targets is not uniform and can be differentially modulated.

5. Conclusions

We found that RVM projections primarily targeted unlabeled dendrites and somata. The absence of GAD67 in the dendritic targets of RVM axon terminals indicates that the targets are not likely to be inhibitory interneurons. However, the present studies did not determine if the target neurons are facilitatory interneurons or projections neurons. Spinal and trigeminal dorsal horns contain neurons projecting to a number of regions that may be involved in nociceptive processing, such as thalamus and the parabrachial nucleus (Mitchell et al., 2004b). Future studies will determine if these projection neurons receive direct synaptic input from RVM descending pathways.

Our finding that approximately two-thirds of RVM projections to lumbar spinal cord are GABAergic are consistent with a recent functional study showing that in 63% of neurons recorded from lumbar spinal dorsal horn, responses to noxious pinch were blocked by electrical stimulation of RVM (Kato et al., 2006). This previous study also showed that either electrical or glutamate stimulation in RVM caused an increase in inhibitory postsynaptic currents (IPSCs) in dorsal horn neurons which were blocked by GABAergic or glycinergic antagonists (Kato et al., 2006). Together these studies support the notion that the RVM projection to spinal dorsal horn is both anatomically and functionally inhibitory.

Furthermore, the demonstration of changes in IPSCs supports the notion that the descending projection directly influences the dorsal horn neurons, rather than the primary afferent terminals. In contrast, our present findings would suggest that a similar analysis in trigeminal dorsal horn would be more likely to reveal facilitation from RVM in at least a subset of nociceptive neurons.

Acknowledgments

Support from NIH grants DE012640 and RR016858 (confocal microscope). The electron microscopy was made possible by an instrumentation grant from the M.J. Murdock Charitable Trust. The authors would like to thank James F. Castano for his technical assistance.

References

Aicher SA, Goldberg A, Sharma S, Pickel VM. μ-Opioid receptors are present in vagal afferents and their dendritic targets in the medial nucleus tractus solitarius. J Comp Neurol. 2000; 422:181–190. [PubMed: 10842226]

Aicher SA, Reis DJ, Nicolae R, Milner TA. Monosynaptic projections from the medullary gigantocellular reticular formation to sympathetic preganglionic neurons in the thoracic spinal cord. J Comp Neurol. 1995; 363:563–580. [PubMed: 8847418]

Alvarez FJ, Kavookjian AM, Light AR. Synaptic interactions between GABA-immunoreactive profiles and the terminals of functionally defined myelinated nociceptors in the monkey and cat spinal cord. J Neurosci. 1992; 12:2901–2917. [PubMed: 1494939]

Alvarez FJ, Kavookjian AM, Light AR. Ultrastructural morphology, synaptic relationships, and CGRP immunoreactivity of physiologically identified C-fiber terminals in the monkey spinal cord. J Comp Neurol. 1993; 329:472–490. [PubMed: 7681070]

Antal M, Petkó M, Polgár E, Heizmann CW, Storm-Mathisen J. Direct evidence of an extensive GABAergic innervation of the spinal dorsal horn by fibres descending from the rostral ventromedial medulla. Neuroscience. 1996; 73:509–518. [PubMed: 8783266]

Bailey TW, Hermes SM, Andresen MC, Aicher SA. Cranial visceral afferent pathways through the nucleus of the solitary tract to caudal ventrolateral medulla or paraventricular hypothalamus: target-specific synaptic reliability and convergence patterns. J Neurosci. 2006; 26:11893–11902. [PubMed: 17108163]

Bereiter DA, Hirata H, Hu JW. Trigeminal subnucleus caudalis: Beyond homologies with the spinal dorsal horn. Pain. 2000; 88:221–224. [PubMed: 11068108]

Bottger P, Tracz Z, Heuck A, Nissen P, Romero-Ramos M, Lykke-Hartmann K. Distribution of Na/K-ATPase alpha 3 isoform, a sodium-potassium P-type pump associated with rapid-onset of dystonia parkinsonism (RDP) in the adult mouse brain. J Comp Neurol. 2011; 519:376–404. [PubMed: 21165980]

Chan J, Aoki C, Pickel VM. Optimization of differential immunogold-silver and peroxidase labeling with maintenance of ultrastructure in brain sections before plastic embedding. J Neurosci Meth. 1990; 33:113–127.

Edelmayer RM, Vanderah TW, Majuta L, Zhang ET, Fioravanti B, De FM, Chichorro JG, Ossipov MH, King T, Lai J, Kori SH, Nelsen AC, Cannon KE, Heinricher MM, Porreca F. Medullary pain facilitating neurons mediate allodynia in headache-related pain. Ann Neurol. 2009; 65:184–193. [PubMed: 19259966]

Fang F, Proudfit HK. Spinal cholinergic and monoamine receptors mediate the antinociceptive effect of morphine microinjected in the periaqueductal gray on the rat tail, but not the feet. Brain Res. 1996; 722:95–108. [PubMed: 8813354]

Fields HL, Basbaum AI. Brainstem control of spinal pain-transmission neurons. Annu Rev Physiol. 1978; 40:217–248. [PubMed: 205165]

Fields HL, Basbaum AI, Clanton CH, Anderson SD. Nucleus raphe magnus inhibition of spinal cord dorsal horn neurons. Brain Res. 1977; 126:441–453. [PubMed: 861731]

Fields HL, Bry J, Hentall I, Zorman G. The activity of neurons in the rostral medulla of the rat during withdrawal from noxious heat. J Neurosci. 1983; 3:2545–2552. [PubMed: 6317812]

Fields HL, Malick A, Burstein R. Dorsal horn projection targets of ON and OFF cells in the rostral ventromedial medulla. J Neurophysiol. 1995; 74:1742–1759. [PubMed: 8989409]

Fong AY, Stornetta RL, Foley CM, Potts JT. Immunohistochemical localization of GAD67-expressing neurons and processes in the rat brainstem: subregional distribution in the nucleus tractus solitarius. J Comp Neurol. 2005; 493:274–290. [PubMed: 16255028]

Guo C, Hirano AA, Stella SL Jr, Bitzer M, Brecha NC. Guinea pig horizontal cells express GABA, the GABA-synthesizing enzyme GAD 65, and the GABA vesicular transporter. J Comp Neurol. 2010; 518:1647–1669. [PubMed: 20235161]

Haber LH, Martin RF, Chung JM, Willis WD. Inhibition and excitation of primate spinothalamic tract neurons by stimulation in region of nucleus reticularis gigantocellularis. J Neurophysiol. 1980; 43:1578–1593. [PubMed: 6251179]

Hargreaves KM. Orofacial pain. Pain. 2011; 152:S25–S32. [PubMed: 21292394]

Hegarty DM, Tonsfeldt K, Hermes SM, Helfand H, Aicher SA. Differential localization of vesicular glutamate transporters and peptides in corneal afferents to trigeminal nucleus caudalis. J Comp Neurol. 2010; 518:3557–3569. [PubMed: 20593358]

Heinricher MM, Barbaro NM, Fields HL. Putative nociceptive modulating neurons in the rostral ventromedial medulla of the rat: firing of on- and off-cells is related to nociceptive responsiveness. Somatosens Mot Res. 1989; 6:427–439. [PubMed: 2547275]

Heinricher MM, Morgan MM, Tortorici V, Fields HL. Disinhibition of off-cells and antinociception produced by an opioid action within the rostral ventromedial medulla. Neuroscience. 1994; 63:279–288. [PubMed: 7898652]

Heusner CL, Beutler LR, Houser CR, Palmiter RD. Deletion of GAD67 in dopamine receptor-1 expressing cells causes specific motor deficits. Genesis. 2008; 46:357–367. [PubMed: 18615733]

Hsu SM, Raine L, Fanger H. Use of avidin-biotin-peroxidase complex (ABC) in immunoperoxidase techniques: A comparison between ABC and unlabeled antibody (PAP) procedures. J Histochem Cytochem. 1981; 29:557–580.

Jones BE, Holmes CJ, Rodriguez-Veiga E, Mainville L. GABA-synthesizing neurons in the medulla: Their relationship to serotonin-containing and spinally projecting neurons in the rat. J Comp Neurol. 1991; 313:349–367. [PubMed: 1722490]

Kalyuzhny AE, Wessendorf MW. Serotonergic and GABAergic neurons in the medial rostral ventral medulla express κ-opioid receptor immunoreactivity. Neuroscience. 1999; 90:229–234. [PubMed: 10188949]

Kato G, Yasaka T, KAtafuchi T, Furue H, Mizuno M, Iwamoto Y, Yoshimura M. Direct GABAergic and glycinergic inhibition of the substantia gelatinosa from the rostral ventromedial medulla revealed by in vivo patch-clamp analysis in rats. J Neurosci. 2006; 26:1787–1794. [PubMed: 16467527]

Light AR, Kavookjian AM. The ultrastructure and synaptic connections of the spinal terminations from single, physiologically characterized axons descending in the dorsolateral funiculus from the midline, pontomedullary region. J Comp Neurol. 1985; 234:549–560. [PubMed: 3988999]

Meng ID, Bereiter DA. Differential distribution of Fos-like immunoreactivity in the spinal trigeminal nucleus after noxious and innocuous thermal and chemical stimulation of rat cornea. Neuroscience. 1996; 72:243–254. [PubMed: 8730721]

Meng ID, Hu JW, Bereiter DA. Parabrachial area and nucleus raphe magnus inhibition of corneal units in rostral and caudal portions of trigeminal subnucleus caudalis in the rat. Pain. 2000; 87:241–251. [PubMed: 10963904]

Millan MJ. Descending control of pain. Prog Neurobiol. 2002; 66:355–474. [PubMed: 12034378]

Millhorn DE, Ho:kfelt T, Seroogy K, Oertel W, Verhofstad AAJ, Wu JY. Immunohistochemical evidence for colocalization of gamma-aminobutyric acid and serotonin in neurons of the ventral medulla oblongota projecting to the spinal cord. Brain Res. 1987; 410:179–185. [PubMed: 3555707]

Mitchell JL, Silverman MB, Aicher SA. Rat trigeminal lamina I neurons that project to thalamic or parabrachial nuclei contain the mu-opioid receptor. Neuroscience. 2004a; 128:571–582. [PubMed: 15381286]

Mitchell JL, Silverman MB, Aicher SA. Rat trigeminal lamina I neurons that project to thalamic or parabrachial nuclei contain the mu-opioid receptor. Neuroscience. 2004b; 128:571–582. [PubMed: 15381286]

Morgan MM, Whittier KL, Hegarty DM, Aicher SA. Periaqueductal gray neurons project to spinally projecting GABAergic neurons in the rostral ventromedial medulla. Pain. 2008; 140:376–386. [PubMed: 18926635]

Mullen RJ, Buck CR, Smith AM. NeuN, a neuronal specific nuclear protein in vertebrates. Development. 1992; 116:201–211. [PubMed: 1483388]

Paxinos G, Watson C. The Rat Brain in Stereotaxic Coordinates. 1998; 4

Pickel VM. Immunocytochemical methods. 1981; 1:483–509.

Pozo MA, Cervero F. Neurons in the rat spinal trigeminal complex driven by corneal nociceptors: Receptive-field properties and effects of noxious stimulation of the cornea. J Neurophysiol. 1993; 70:2370–2378. [PubMed: 8120588]

Ruda MA, Bennett GJ, Dubner R. Neurochemistry and neural circuitry in the dorsal horn. Prog Brain Res. 1986; 66:219–268. [PubMed: 3538168]

Sandkühler J, Gebhart GF. Characterization of inhibition of a spinal nociceptive reflex by stimulation medially and laterally in the midbrain and medulla in the pentobarbital-anesthetized rat. Brain Res. 1984; 305:67–76. [PubMed: 6744062]

Silverman MB, Hermes SM, Zadina JE, Aicher SA. Mu-opioid receptor is present in dendritic targets of Endomorphin-2 axon terminals in the nuclei of the solitary tract. Neuroscience. 2005; 135:887–896. [PubMed: 16154285]

Strassman AM, Vos BP. Somatotopic and laminar organization of fos-like immunoreactivity in the medullary and upper cervical dorsal horn induced by noxious facial stimulation in the rat. J Comp Neurol. 1993; 331:495–516. [PubMed: 8509507]

Urban MO, Zahn PK, Gebhart GF. Descending facilitatory influences from the rostral medial medulla mediate secondary, but not primary hyperalgesia in the rat. Neuroscience. 1999; 90:349–352. [PubMed: 10215139]

Winkler CW, Hermes SM, Chavkin CI, Drake CT, Morrison SF, Aicher SA. Kappa opioid receptor (KOR) and GAD67 immunoreactivity are found in OFF and NEUTRAL cells in the rostral ventromedial medulla. J Neurophysiol. 2006; 96:3465–3473. [PubMed: 17005613]

Zhuo M, Gebhart GF. Characterization of descending inhibition and facilitation from the nuclei reticularis gigantocellularis and gigantocellularis pars alpha in the rat. Pain. 1990; 42:337–350. [PubMed: 1979161]

Highlights

We find distinctions between RVM projections to spinal versus trigeminal dorsal horn.

Projections to spinal dorsal horn are more likely to contain GAD67.

Projections to spinal dorsal horn are more likely to contact NeuN-labeled somata.

Descending afferents may underlie segmental differences in nociceptive processing.

Ethical Statement

All protocols were approved by the Institutional Animal Care and Use Committee at Oregon Health & Science University and conform to the European Union Directive 2010/63/EU for animal experimentation.

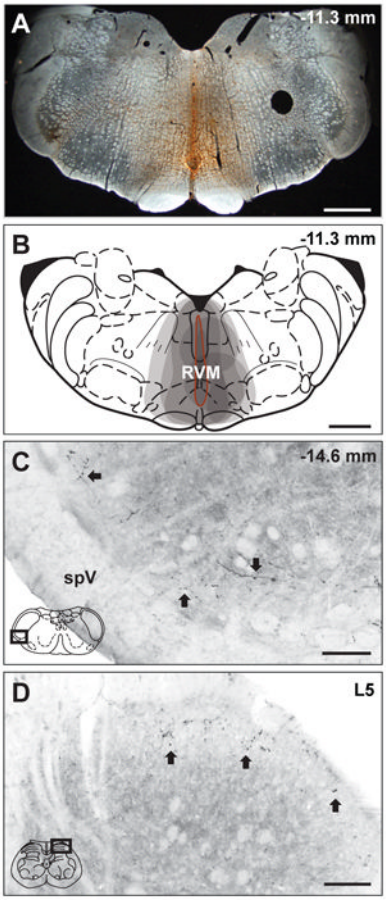

Figure 1.

BDA injections into RVM produce anterograde labeling in trigeminal and spinal dorsal horns. (A) A representative micrograph of a BDA injection site in RVM and (B) a composite schematic illustrating individual BDA injections into RVM. (B) Each injection site is indicated by a grey shaded area, thus the darker regions represent areas included in multiple injections. All injections included the ventromedial medulla and all BDA injections into RVM resulted in bilateral labeling. The injection site outlined in red (B) represents the BDA injection site in the representative micrograph (A). (C) BDA labeling is present in representative micrographs in trigeminal (C) and spinal (C) dorsal horns. (C) BDA-labeled reticulomedullary projections were observed throughout the rostrocaudal extent of the trigeminal dorsal horn from Vi/Vc to Vc/C1 in laminae I and II as fibers with distinct varicosities (Arrows). (D) BDA-labeled reticulospinal projections were also observed as fibers and varicosities (Arrows) in laminae I and II of the lumbar spinal cord. The representative diagrams of the RVM (B), the trigeminal brainstem (C) and the spinal cord (D) are modified from the digital rat atlas of Paxinos and Watson (Paxinos and Watson, 1998) and are reproduced here with permission from the publisher. The dark rectangles in panels C and D represent the respective locations of each micrograph. The numbers on the upper right side of panels A, B and C represent the distance from bregma. In panel D, L5 refers to lumbar level 5 of the spinal cord. Scale bars: panels A and B = 1 mm; panels C and D = 100 μm. spV, spinal trigeminal tract.

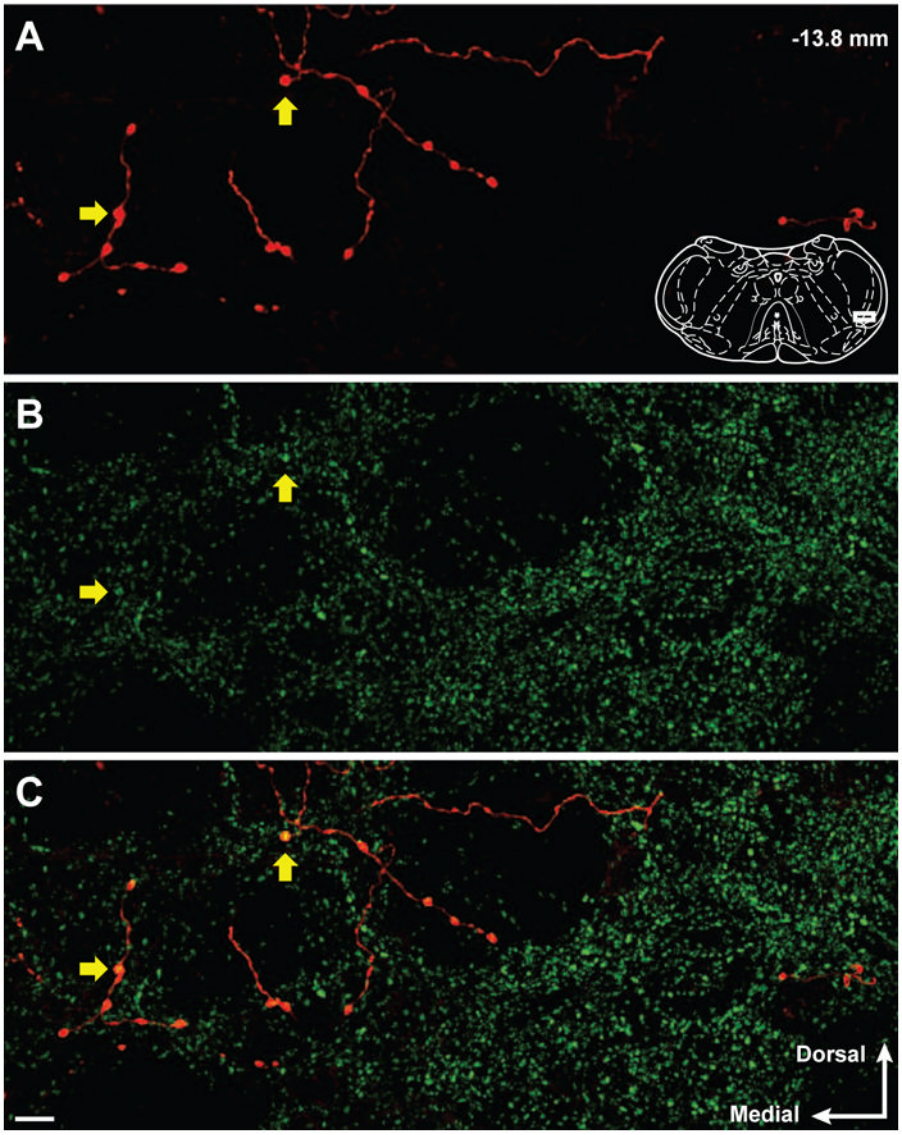

Figure 2.

Confocal micrographs show BDA-labeled reticulomedullary varicosities and GAD67 immunoreactivity in the trigeminal dorsal horn. (A) Reticulomedullary projections display axonal labeling with distinct varicosities. (B) GAD67 immunoreactivity in the trigeminal dorsal horn is abundant and predominantly punctate. (C) Overlay of panels A and B illustrate several BDA-labeled reticulospinal varicosities that contain GAD67 immunoreactivity (Yellow arrows). The representative diagram of the trigeminal brainstem in panel A is modified from the digital rat atlas of Paxinos and Watson (Paxinos and Watson, 1998) and is reproduced here with permission from the publisher. The white rectangle on the diagram in panel A represents the location of the micrographs. The number in the upper right of panel A represents the distance from bregma. The white arrows in the lower right of panel C represent the medial and dorsal orientation of the micrographs. Micrographs are 14 consecutive and overlapping optical sections composing a 6.5 um thick Z stack. Scale bar = 10 um.

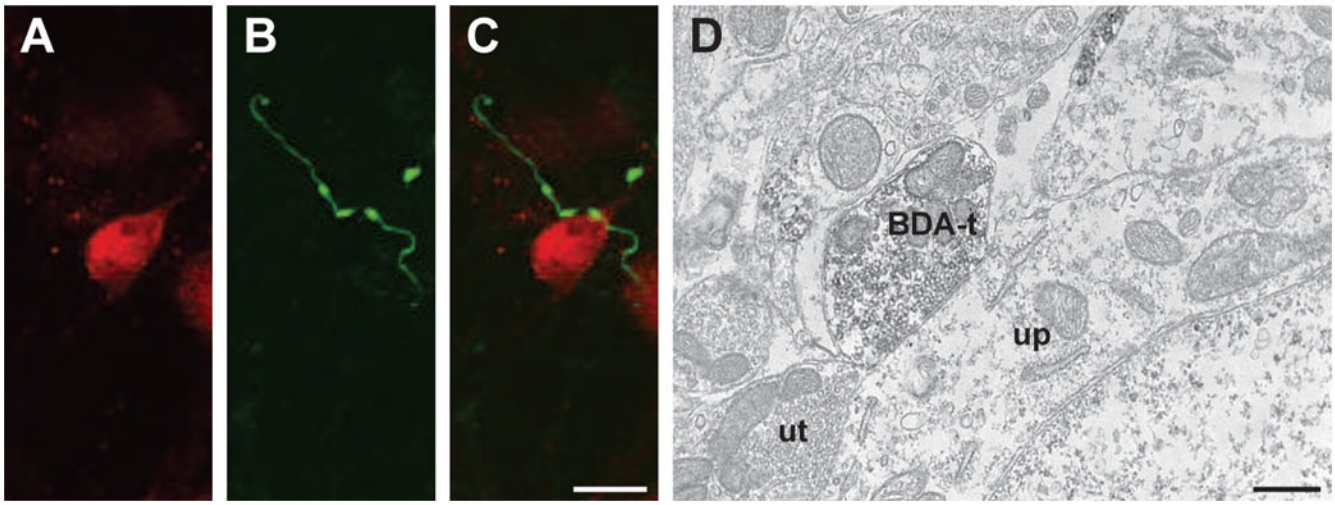

Figure 3.

Reticulomedullary and reticulospinal terminals were observed contacting neurons with confocal (A-C) and electron (D) microscopy. (A-C) Confocal micrographs (10 consecutive and overlapping optical sections composing a 4.5 um thick Z stack) illustrate (A) a NeuN-ir neuron and (B) BDA-labeled reticulomedullary varicosities in the trigeminal dorsal horn. (C) The overlay demonstrates appositions between two BDA-labeled reticulomedullary varicosities and the NeuN-ir cell. Scale bar = 10 um for panels A - C. (D) Electron micrograph illustrating a BDA-labeled terminal (BDA-t) forming an apposition with an unlabeled perikarya (up). An unlabeled terminal (ut) is also seen forming an apposition with the cell. Scale bar = 500 nm.

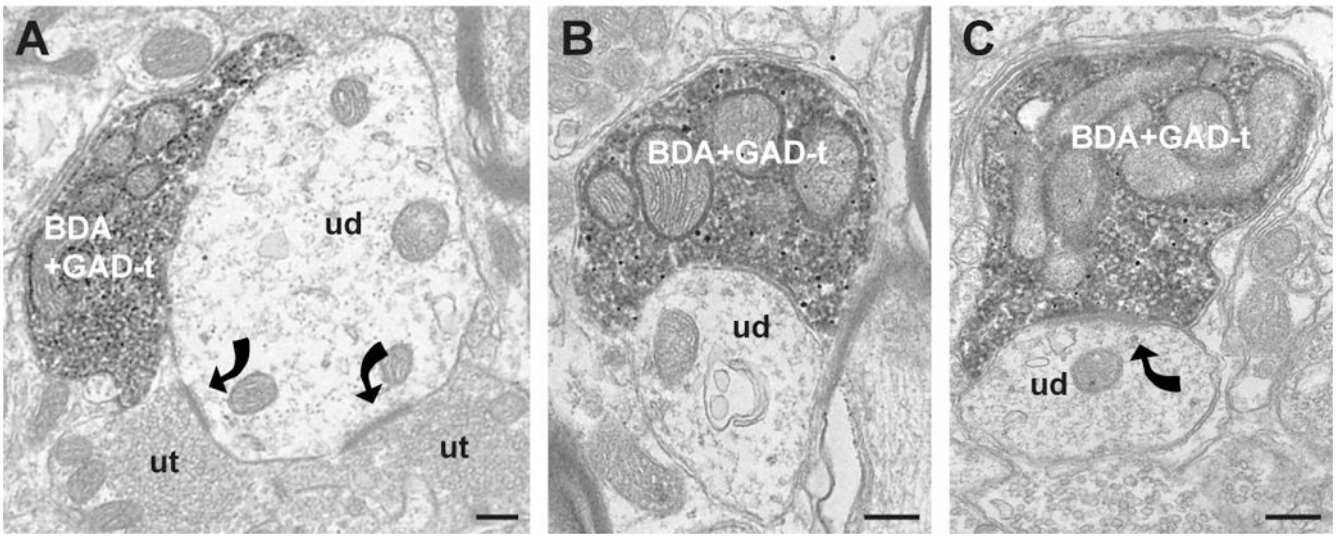

Figure 4.

Electron micrographs illustrate the frequently observed types of contacts seen between GABAergic reticulomedullary (A, B) and reticulospinal terminals (C) onto unlabeled dendrites. (A) A GAD67-ir BDA-labeled reticulomedullary terminal (BDA+GAD-t) contacts a large unlabeled dendrite (ud). The dendrite also receives asymmetric synapses (curved arrows) from two unlabeled axon terminals (ut). (B) A small unlabeled dendrite (ud) receives an apposition from a GAD67-ir reticulomedullary terminal (BDA+GAD-t) in the trigeminal dorsal horn. (C) Also the most common interaction seen in the lumbar dorsal horn, a GAD67-ir BDA-labeled terminal (BDA+GAD-t) forms a symmetric synapse (curved arrow) with an unlabeled dendrite (ud). All scale bars = 250 nm.

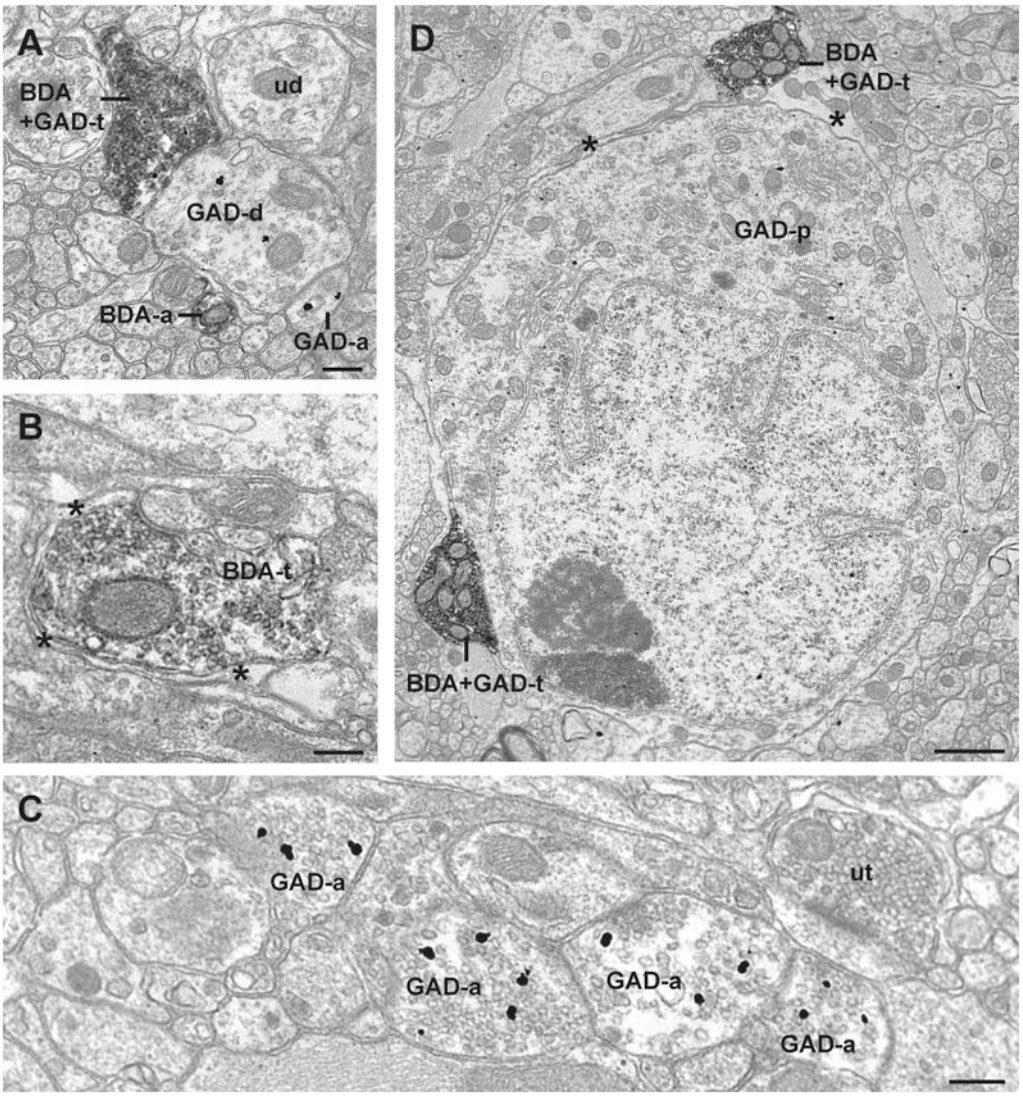

Figure 5.

Electron micrographs illustrate less common occurrences of BDA and GAD67 immunoreactivity in the trigeminal (A-C) and lumbar (D) dorsal horns. (A) A GAD67-ir BDA-labeled reticulomedullary terminal (BDA+GAD-t) contacts a GAD67-ir dendrite (GAD-d). A BDA-labeled axon (BDA-a), a GAD67-ir axon (GAD-a), and an unlabeled dendrite (ud) are also seen in the image. (B) A BDA-labeled reticulomedullary terminal (BDA-t) is largely surrounded by a astrocytic glial processes (asterisks). (C) GAD67-ir axons (GAD-a) and an unlabeled terminal (ut). (D) Two GAD67-ir BDA-labeled reticulospinal terminals (BDA+GAD-t) are seen in proximity to a GAD67-ir cell (GAD-p). The terminal at the bottom left of the image is in contact with the cell while the terminal in the upper right is separated by a glial sheath (asterisk). Scale bars for panels A-C = 250 nm, and the scale bar for panel D = 1 um.

Table 1

Summary of ultrastructural interactions between RVM projections to trigeminal and lumbar spinal dorsal horns.

BDA Labeled Terminals		Target					
		GAD + Dendrite	**GAD – Dendrite**	**GAD + Soma**	**GAD – Soma**	**Other**	**Total**
Trigeminal	GAD + Terminal	2 (6%)	23 (70%)	0 (0%)	0 (0%)	8 (24%)	33
	GAD -Terminal	0 (0%)	10 (56%)	0 (0%)	1 (6%)	7 (39%)	18
Lumbar	GAD + Terminal	1 (4%)	11 (48%)	2 (9%)	0 (0%)	9 (39%)	23
	GAD -Terminal	1 (8%)	7 (54%)	0 (0%)	1 (8%)	4 (31%)	13
Total	GAD + Terminal	3 (5%)	34 (61%)	2 (4%)	0	17 (30%)	56
	GAD -Terminal	1 (3%)	17 (55%)	0 (0%)	2 (6%)	11 (35%)	31

Percentages are additive across each row and may not add up to 100% due to rounding.